Molecular Cell, Vol. 18, 735–748, June 10, 2005, Copyright ©2005 by Elsevier Inc. DOI 10.1016/j.molcel.2005.05.003

Intrinsic Histone-DNA Interactions and Low Nucleosome Density Are Important for Preferential Accessibility of Promoter Regions in Yeast

Edward A. Sekinger, Zarmik Moqtaderi, and Kevin Struhl*
Department of Biological Chemistry and Molecular Pharmacology
Harvard Medical School
Boston, Massachusetts 02115

Summary

In yeast cells, preferential accessibility of the *HIS3-PET56* promoter region is determined by a general property of the DNA sequence, not by defined sequence elements. In vivo, this region is largely devoid of nucleosomes, and accessibility is directly related to reduced histone density. The *HIS3-PET56* and *DED1* promoter regions associate poorly with histones in vitro, indicating that intrinsic nucleosome stability is a major determinant of preferential accessibility. Specific and genome-wide analyses indicate that low nucleosome density is a very common feature of yeast promoter regions that correlates poorly with transcriptional activation. Thus, the yeast genome is organized into structurally distinct promoter and nonpromoter regions whose DNA sequences inherently differ with respect to nucleosome formation. This organization ensures that transcription factors bind preferentially to appropriate sites in promoters, rather than to the excess of irrelevant sites in nonpromoter regions.

Introduction

In eukaryotic organisms, promoter accessibility and gene regulation are influenced by chromatin. There are at least five general mechanisms for altering chromatin structure and affecting the accessibility of the underlying DNA to the nuclear environment. First, during S phase, the newly synthesized DNA helices initially inherit only the parental histones, thereby temporarily revealing half of the DNA to nuclear proteins. Second, nucleosome-remodeling complexes (e.g., SWI/SNF and RSC) can slide or displace histone octamers in an ATP-dependent fashion, thereby increasing the association of transcription factors to DNA (Becker and Horz, 2002; Narlikar et al., 2002; Martens and Winston, 2003). Third, acetylation of the histone N-terminal tails can influence the accessibility of DNA within chromatin (Lee et al., 1993; Vettese-Dadey et al., 1996; Ura et al., 1997; Anderson et al., 2001; Sewack et al., 2001). Fourth, activator proteins can cause dissociation of histones from promoter regions (Deckert and Struhl, 2001; Boeger et al., 2003; Reinke and Horz, 2003; Boeger et al., 2004; Korber et al., 2004). Fifth, transcriptional elongation appears to disrupt nucleosomes throughout the entire protein-coding region (Kristjuhan and Svejstrup, 2004; Lee et al., 2004; Schwabish and Struhl, 2004), and the FACT and Spt6 complexes are important to restore normal chromatin structure and prevent inappropriate initiation within protein-coding regions (Formosa et al., 2002; Belotserkovskaya et al., 2003; Kaplan et al., 2003; Mason and Struhl, 2003). As a consequence of activator- and elongation-mediated eviction of histones, nucleosome depletion is observed at transcriptionally active regions throughout the entire yeast genome (Lee et al., 2004).

In the yeast *Saccharomyces cerevisiae*, promoter regions in the context of chromatin are generally more accessible to nuclear proteins than protein-coding regions. A number of yeast promoters contain transcription-independent regions of nuclease hypersensitivity, and the Ty1 retrotransposon preferentially integrates in promoter regions (see Mai et al. [2000] for references). Of more biological significance, the binding of transcriptional regulatory proteins to their target DNA sequences is largely restricted to intergenic regions. For example, genome-wide analysis reveals specific binding of Rap1 to promoters, even though consensus Rap1 binding sites reside within the coding sequences of many genes (Lieb et al., 2001). Similarly, Gcn4 binds preferentially to target sequences in promoters (Kuo et al., 2000), which is important because most Gcn4 consensus sequences are in protein-coding regions, and the number of potential Gcn4 binding sites in the yeast genome far exceeds the number of Gcn4 molecules/cell. In accord with these observations on protein accessibility, promoter and nonpromoter regions of yeast chromatin can be fractionated by physical means (Nagy et al., 2003), indicating that these two classes of genomic sequences are structurally distinct.

Detailed analysis of the divergent *HIS3-PET56* promoter region indicates that preferential accessibility is locally determined by the DNA sequence but does not depend on specific elements such as the Gcn4 binding site, poly(dA:dT) tracts, TATA elements, or initiator elements (Mai et al., 2000). As such, preferential accessibility at this locus cannot be explained by activator-mediated eviction of nucleosomes. Preferential accessibility is also independent of the SWI/SNF nucleosome-remodeling complex, Gcn5 histone acetylase complexes, and ubiquitination of histone H2B. Strikingly, progressive deletion of the *HIS3-PET56* promoter region in either direction results in a progressive loss of accessibility, indicating that multiple sequence determinants over a 100–200 bp region are involved in preferential accessibility. Thus, preferential accessibility of the *HIS3-PET56* (and presumably other) promoter region is determined by a general property of the DNA sequence rather than by defined sequence elements (Mai et al., 2000). However, the mechanisms by which the *HIS3-PET56* and other promoters are preferentially accessible are unknown.

Here, we investigate the mechanistic basis for preferential accessibility of the *HIS3-PET56* promoter region. By using a novel nucleosome-scanning assay, as well as direct measurements of histone density, we show that the accessible region is largely devoid of nucleosomes in vivo. This pattern of nucleosome occupancy

*Correspondence: kevin@hms.harvard.edu

in *S. cerevisiae* can be largely reproduced in vitro with purified histones and DNA as well as in the evolutionarily distant yeast *Schizosaccharomyces pombe*. These observations demonstrate that low nucleosome density due to intrinsically poor nucleosome stability is is a major determinant of preferential accessibility of the *HIS3-PET56* promoter region. Similarity, low histone density at the *DED1* promoter is reproduced in vitro and, hence, is due to intrinsic histone-DNA interactions. Specific and genome-wide analyses indicate that low nucleosome density is a very common, although not universal, feature of yeast promoter regions. Thus, the yeast genome is organized into distinct promoter and nonpromoter regions whose DNA sequences inherently differ with respect to nucleosome formation, thereby permitting transcription factors to bind preferentially to appropriate sites in promoters.

Results

Alteration of the *HIS3-PET56* Intergenic Region Has Limited Effects on the Positions of Flanking Nucleosomes in the Coding Regions

As assayed by HinfI cleavage in vivo in yeast strains containing wild-type (wt) or deleted versions of the divergent *HIS3-PET56* promoter region, preferential accessibility is determined by a general property of the DNA sequence, not by specific elements (Mai et al., 2000). As a first step to explore the structural basis for this preferential accessibility, we used micrococcal nuclease (MNase) to examine the chromatin structure of this region in wt and mutant strains. In accord with previous results (Struhl, 1982; Oettinger and Struhl, 1985; Losa et al., 1990), low-resolution (Southern blotting) analysis of the wt strain reveals positioned nucleosomes within the *HIS3* and *PET56* coding regions and two sites of significant MNase cleavage in the promoter region (Figure 1A, lanes 5 and 6). High-resolution (nucleotide level) analysis identifies the localized digestion to the positions –70 and –190 with respect to the *HIS3* ATG initiation codon (Figure 1B). It is difficult to determine whether MNase cleavage at positions –70 and –190 define boundaries of positioned nucleosomes that cover the 5′-proximal portions of the *HIS3* and *PET56* coding regions, because both sites are also preferentially cleaved in purified DNA.

In three strains containing significant deletions in the *HIS3-PET56* promoter region, the nucleosomal arrays within the *HIS3* and *PET56* coding regions are positioned similarly to that observed in the wt strain (Figure 1A; compare lanes 5 and 6 with lanes 9 and 10, 13 and 14, and 17 and 18). Analysis at the nucleotide level (data not shown) and "nucleosome-scanning" experiments (see below) corroborate these results, although subtle alterations may occur. Thus, the intergenic region does not dictate the positioning of flanking nucleosomes in the coding region, suggesting that the sequences within the *HIS3* and *PET56* coding regions are important for determining nucleosome positions.

The Divergent *HIS3-PET56* Promoter Region Is Largely Devoid of Nucleosomes

Standard MNase mapping as employed here can identify positioned nucleosomes, but it does not easily distinguish whether a given DNA region is occupied by randomly positioned nucleosomes or no nucleosomes. Furthermore, even when positioned nucleosomes are identified, it is difficult to determine the percentage of chromosomes that have a nucleosome at this position. We therefore developed a nucleosome-scanning method for mapping nucleosomes and determining nucleosome density in a quantitative manner. Specifically, chromatin and purified genomic DNA are lightly digested with MNase, and mononucleosomal-sized DNA fragments (140–220 bp) are isolated by gel electrophoresis (Figure 2A, gel inset). The resulting DNA samples are amplified with overlapping primer pairs (typically in 30 bp intervals) that generate products of similar size (100 ± 8 bp). Nucleosome density of a given region is defined by the ratio of DNA in the chromatin versus purified DNA samples.

The results of such a nucleosome-scanning experiment are interpreted as follows. First, if a nucleosome is perfectly positioned (i.e., present at that position in all cells), a primer pair located totally within this nucleosome will yield a maximal histone density that can be defined as 100%. On the other hand, if one primer is within and the other primer is outside the nucleosome, the apparent nucleosome density will be zero. Thus, a positioned nucleosomal array will generate peaks and valleys, with the valleys corresponding to linker regions between nucleosomes. A similar pattern will arise if only a fraction of cells contain a positioned nucleosome, but the difference in magnitude between the peaks and valleys will be reduced. Second, a region occupied by randomly positioned nucleosomes should display a relatively constant level of nucleosome density that is ~30% of the maximal level. Third, a region deficient in nucleosomes should display low density over the entire region.

To validate this nucleosome-scanning assay, we examined the chromatin structure of the *PHO5* promoter region, which contains four well-positioned nucleosomes under standard (high-phosphate) growth conditions. As shown in Figure 2A, we observed two strongly positioned nucleosomes that correspond well to nucleosomes –1 and –2, which have been described previously. The 8-fold difference between the peak and trough of nucleosome density indicates that a high percentage of cells contain positioned nucleosomes in this region. We also observed positioned nucleosomes within the *PHO5* coding region (previously defined as +1 and +2), but the relatively small difference between the peaks and troughs suggest that these nucleosomes are less well positioned.

Analysis of the *HIS3-PET56* region reveals an array of three positioned nucleosomes within the initial 430 bp of the *HIS3* coding region and a positioned nucleosome at the 5′ region of the adjacent *PET56* coding region (Figure 2B). *HIS3* nucleosomes B and C show a maximal density that is ~40% of that observed for *PHO5*, suggesting that these nucleosomes are well positioned but perhaps not in all cells at any given moment. *HIS3* nucleosome A and the *PET56* nucleosome show significantly lower maximal density, but there is a clear difference between the peaks and valleys. The simplest interpretation of this observation is that these nucleosomes at the beginning of the *HIS3* and *PET56*

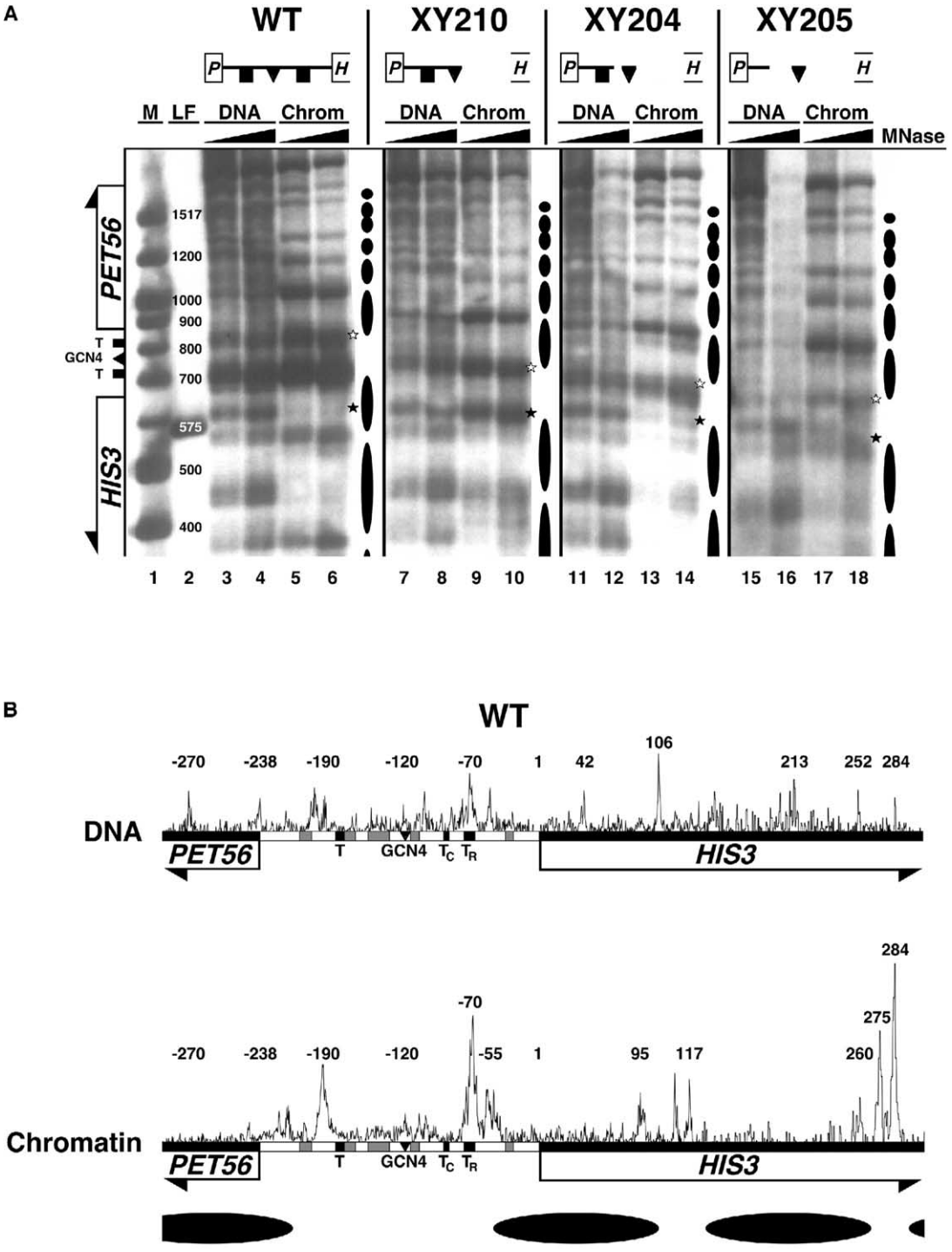

Figure 1. Progressive Deletion of the *his3-pet56* Intergenic Region Does Not Cause Major Changes in Nucleosome Position within the Flanking Coding Regions

(A) MNase-digested chromatin (Chrom) and genomic DNA from wild-type (wt) was analyzed by Southern blotting using a *HIS3* probe. The *PET56* (*P*) and *HIS3* (*H*) coding regions are divergently transcribed from core promoters (black boxes) that are downstream from the Gcn4 binding site (solid triangles). The inferred positions of nucleosomes (solid ovals) are shown with respect to the *PET56* core promoter (open stars) and the *HIS3* deletion junction (+18; solid stars); cleavage sites were mapped by using a landmark fragment (LF) corresponding to cleavage at the HinfI site at +48 and molecular weight markers (M).

(B) MNase-digested chromatin and purified genomic DNAs were analyzed by amplified primer extension at nucleotide resolution, and the data are depicted as a densitometric scan of the lower-strand DNA profile (normalized to position –120). Preferred MNase cleavage sites and other relevant sites are indicated with respect to the *HIS3* T_C and T_R and *PET56* (T) TATA elements (black boxes), poly(dA:dT) tracts (shaded boxes), and Gcn4 binding site.

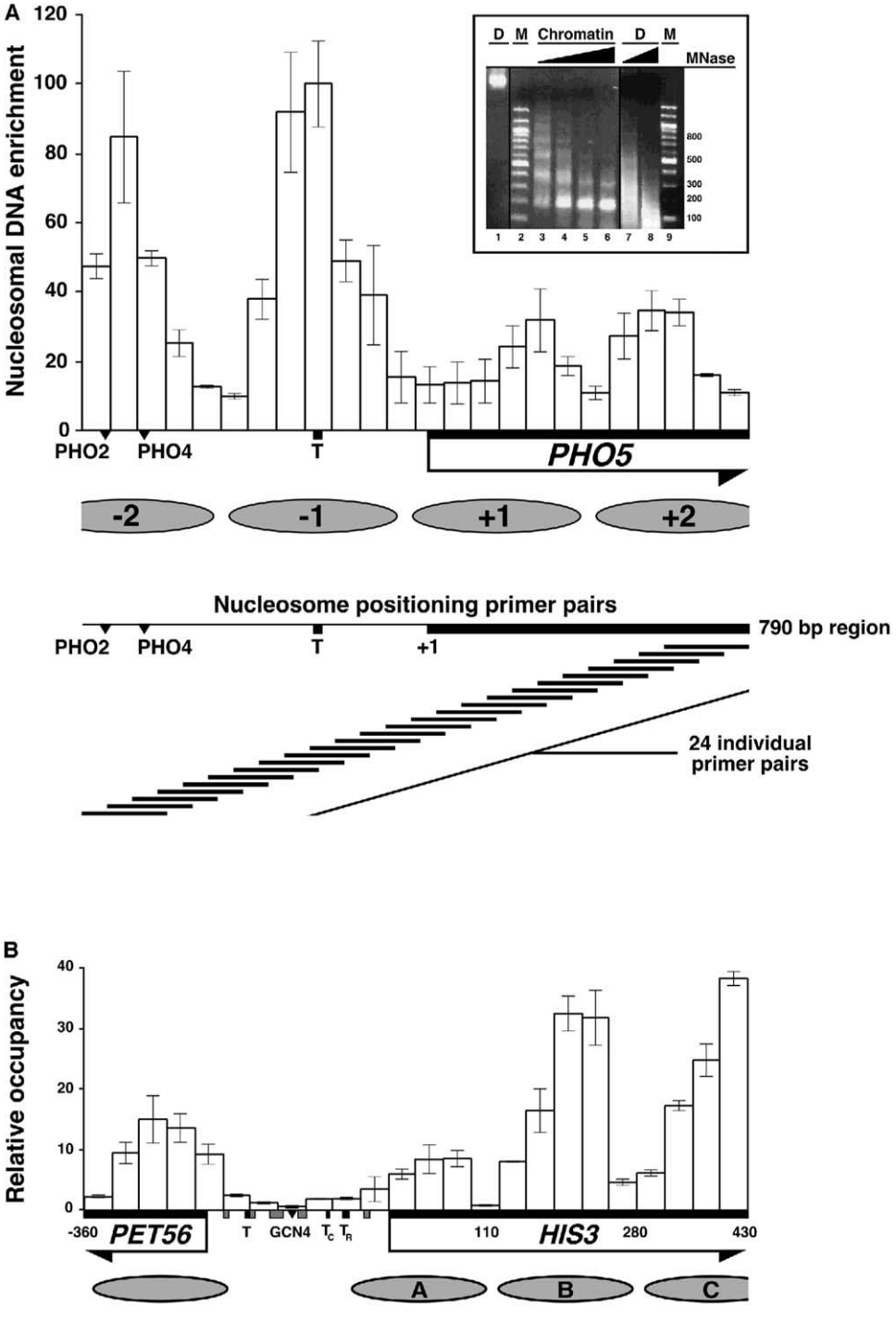

Figure 2. Nucleosome-Scanning Analysis Indicates that the *HIS3-PET56* Promoter Region Is Largely Devoid of Nucleosomes

(A) Nucleosomal DNA enrichment at the indicated positions of the *PHO5* locus with respect to inferred locations of nucleosomes numbered as described previously (shaded ovals), mRNA coding sequence (arrowed line), Pho2 and Pho4 binding sites, and core promoter (T). Inset, agarose gel illustrating MNase-digested chromatin and genomic DNA (D).

(B) Nucleosome enrichment at the divergent *HIS3-PET56* promoter. Values are normalized with respect to the *PHO5* core promoter region (defined as 100) in the same sample.

Data are presented as the average of three independent experiments along with the SEM.

coding regions are positioned in a relatively small fraction of cells and that a significant fraction of cells do not have nucleosomes in this location. Most importantly, the entire *HIS3-PET56* promoter region is extremely deficient in nucleosomes. Thus, the region of preferential accessibility is largely devoid of nucleosomes, and it is

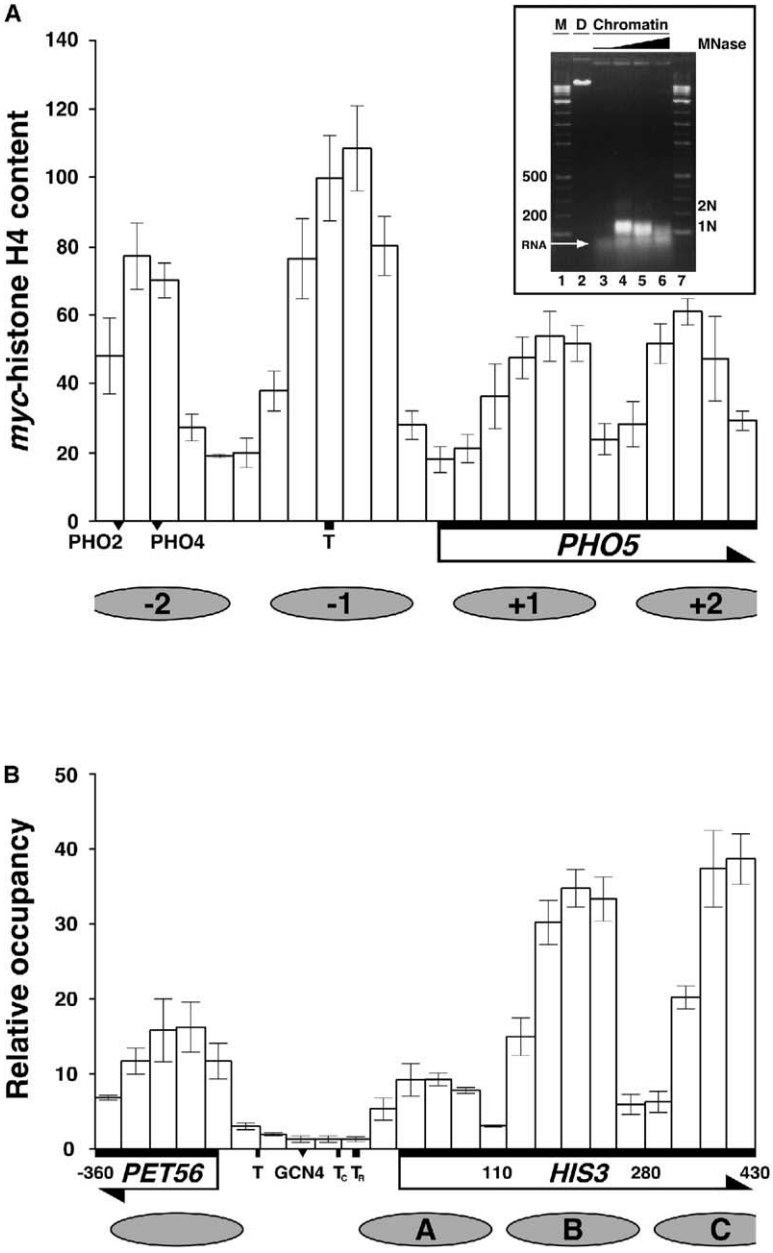

Figure 3. Analysis of Histone H4 Content at the *HIS3-PET56* Region

Crosslinked chromatin from a strain expressing myc-H4 was extensively treated with MNase to generate mononucleosomes (see inset; lane 2 is genomic DNA), and the resulting material (lane 5) was immunoprecipitated with an antibody against the Myc epitope. H4 content for the indicated regions of *PHO5* (top) and *HIS3-PET56* (bottom) are shown, with the *PHO5* TATA region defined as 100. Data are presented as the average of three independent experiments along with the SEM.

possible that a region of reduced nucleosome density spreads beyond the divergent promoter region (see below).

To provide independent evidence for low nucleosome density at the *HIS3-PET56* promoter region, we used chromatin immunoprecipitation (ChIP) to measure occupancy by histone H4 (tagged with the Myc epitope). Crosslinked chromatin was digested with sufficient MNase to generate mononucleosomes lacking the spacer region, in which the length of protected DNA is ~146 bp (Figure 3A, gel inset). At the *PHO5* promoter region, the pattern of histone H4 occupancy is extremely similar to that of nucleosomes defined by the nucleosome-scanning assay (Figure 3A) and to previous descriptions of the region. However, nucleosomes within the *PHO5* coding region appear slightly better positioned when assayed by histone H4 occupancy (compare Figures 3A and 2A). Importantly, the pattern of histone H4 occupancy at the *HIS3-PET56* region is strikingly similar to that observed with the nucleosome-scanning method (Figure 3B). Thus, two independent methods for determining nucleosomal density and positioning at the *HIS3-PET56* region demonstrate that the promoter region is very deficient in nucleosomes when compared to the flanking coding sequences.

Deletions of the *HIS3-PET56* Promoter Region Alter the Pattern of Histone Density

Progressive deletion of the promoter region in either direction results in a progressive loss of accessibility to

HinfI cleavage in vivo (Mai et al., 2000). By using the nucleosome-scanning assay, we examined histone density and positioning in strains containing deletions in the *HIS3-PET56* region that have been previously characterized for HinfI accessibility (Figure 4). In accord with the low-resolution mapping (Figure 1), the positions of *HIS3* nucleosomes B and C as well as the *PET56* nucleosome are minimally affected by the deletions. However, as seen by the decreased distinction between peaks and troughs, the positions of nucleosomes B and (to a lesser extent) C become increasingly randomized as the size of the deletion increases; the *PET56* nucleosome is largely unaffected. The deletions remove much of the sequence corresponding to *HIS3* nucleosome A, but positioned nucleosomes at the equivalent location are not observed in the deletion strains. Most importantly, histone density in the remaining *HIS3-PET56* promoter region gradually increases in a manner that correlates with increased extent of the deletion. Specifically, average histone densities based on the five relevant measurements in the promoter region are 1.2% (wt), 3.0% (XY210), 3.6% (XY204), and 4.8% (XY205). In the most extreme case (XY205), histone density in the *HIS3-PET56* promoter region is only slightly lower than observed at the *PET56* and *HIS3* B nucleosomes (Figure 4), and this derivative shows only slight preferential HinfI cleavage (Mai et al., 2000). Thus, there is a direct relationship between nucleosome occupancy and the level of HinfI accessibility in vivo.

Nucleosome Density and Positioning at the *HIS3-PET56* Region Are Largely Determined by the Intrinsic DNA Sequence Preferences of Histones

In principle, the paucity of nucleosomes in the *HIS3-PET56* promoter region might reflect (1) intrinsic preferences of histones for particular DNA sequences or (2) properties of nucleosome remodeling complexes (or other chromatin-modifying activities) that govern the positions of nucleosomes in vivo. To address this question, we examined whether the pattern of nucleosome density and positioning at the *HIS3-PET56* region could be generated in vitro by using purified histones and DNA. Core histones from HeLa cells were assembled on a 2.8 kb *HIS3-PET56* DNA fragment by gradient salt dialysis, and the resulting nucleosomes were digested with MNase and resolved on an agarose gel (Figure 5A, inset). Mononucleosomal and corresponding genomic DNA were gel purified and analyzed with the same primer pairs used to map the position and density of nucleosomes in vivo.

The pattern of nucleosomes assembled on the *HIS3-PET56* region in vitro (Figure 5A) is strikingly similar to that observed in vivo (Figure 2B). The divergent promoter region is clearly deficient in nucleosomes, and there also appears to be reduced nucleosome density at the 5′-proximal part of the coding region. In addition, the nucleosome at the 5′-proximal part of the *PET56* coding region is positioned similarly to that which occurs in vivo. Interestingly, the nucleosomal array within the *HIS3* coding region appears to have shifted ~40–50 bp upstream from the major position in vivo. This suggests that a nucleosome-remodeling complex is involved in establishing preferred nucleosome positions in the *HIS3* coding region in yeast cells. Most importantly, the fact that low nucleosome density of the *HIS3-PET56* promoter region in vivo can be produced in vitro with purified histones and DNA demonstrates that intrinsic preferences of histones for DNA sequences is responsible for this "nucleosome-free" and preferentially accessible region.

The *S. cerevisiae HIS3-PET56* Promoter Region Has Reduced Histone Density When Examined in *S. pombe* Cells

To provide independent evidence that nucleosome deficiency in the *HIS3-PET56* promoter region is largely determined by intrinsic preferences of histones for DNA, we examined the nucleosome pattern of this *S. cerevisiae* segment of DNA when present in cells of an evolutionarily distant yeast species, *Schizosaccharomyces pombe*. As assayed by nucleosome scanning, the *HIS3-PET56* promoter region has dramatically reduced levels of nucleosomes, and the nucleosome over the *PET56* coding region is positioned similarly to that observed in *S. cerevisiae* cells and in vitro (Figure 5B). However, nucleosomal positioning over the *HIS3* coding region in *S. pombe* cells differs from that observed in *S. cerevisiae* and in vitro. Instead of three positioned nucleosomes, only two exist, and the region of protection appears to be larger or diffuse, suggesting the nucleosomes may not be as tightly packaged and/or may occupy multiple positions. These observations suggest that, unlike the case for the *PET56* nucleosome, precise positioning of nucleosomes over the *HIS3* coding region in *S. pombe* is not simply determined by intrinsic DNA sequence preferences of histones. However, the very low nucleosome density at the promoter region in *S. cerevisiae*, *S. pombe*, and in vitro is predominantly due to properties of the DNA sequence that are inherently undesirable for stable association with histones.

Intrinsic Histone-DNA Interactions also Account for Low Nucleosome Density at the *DED1* Promoter Region

To address whether intrinsic histone-DNA interactions account for low histone density at another yeast promoter region, we examined the *DED1* promoter and flanking regions with the identical samples used to analyze the *HIS3-PET56* region in vivo (Figure 2B) and in vitro (Figure 5A). The *DED1* promoter, which is adjacent to the 3′ end of the *HIS3* coding region, can stimulate transcription of a heterologous RNA polymerase, presumably by increasing its accessibility to the DNA (Chen et al., 1987). As observed for *HIS3-PET56*, the pattern of nucleosomes assembled on the *DED1* region in vitro (Figure 6A) is very similar, although not identical, to that observed in vivo (Figure 6B). Specifically, the *DED1* promoter region is deficient in nucleosomes, and the flanking nucleosome at the 3′ end of the *HIS3* coding region is positioned similarly in vivo and in vitro. The region of low histone density at the *DED1* promoter appears more extended in vitro, such that the proximal nucleosome covering the *DED1* coding sequence (nucleosome E) is difficult to discern. Reconstituted nucleosomes F and G within the *DED1* coding region appear to have

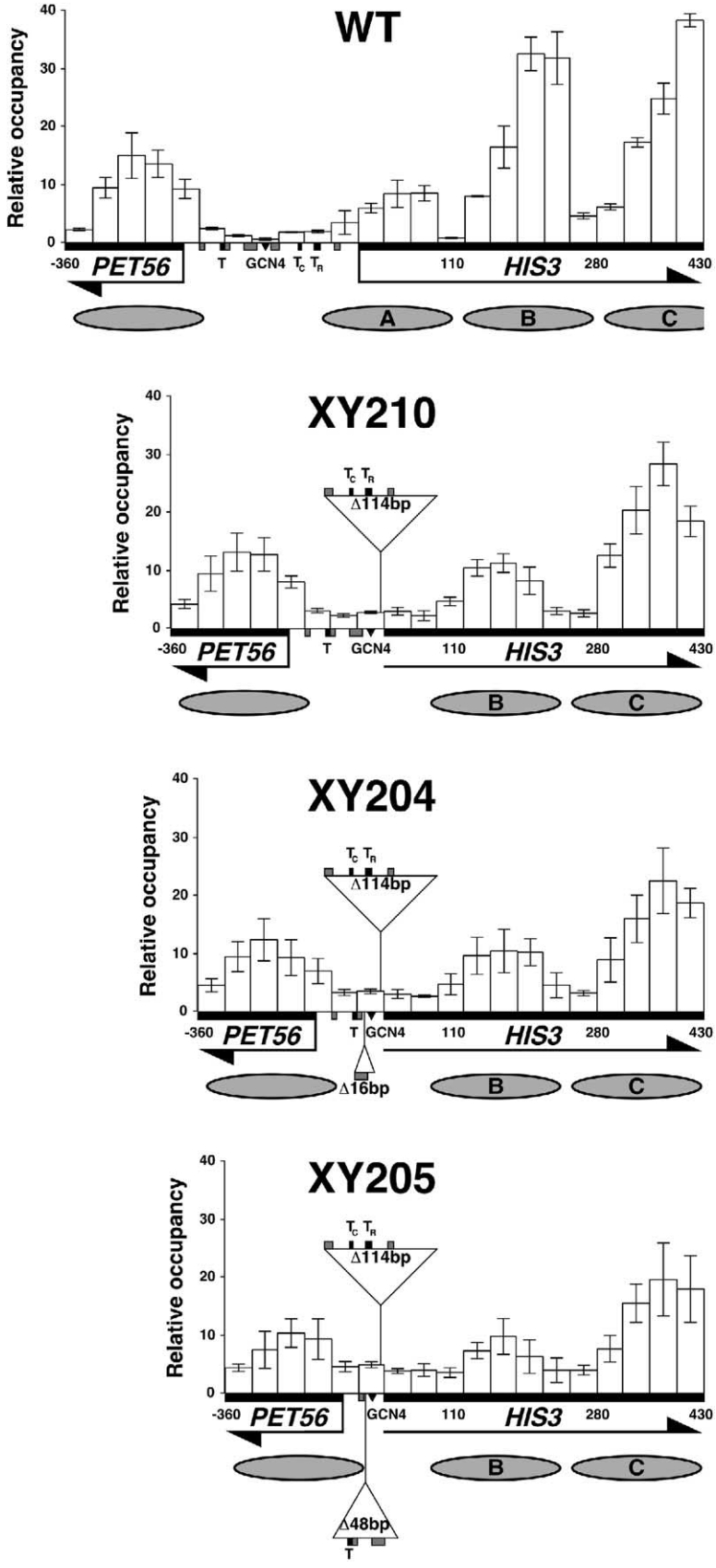

Figure 4. Altered Nucleosome Density in *his3* Promoter Derivatives

Nucleosome-scanning analysis of wt and the indicated deletions in the *HIS3-PET56* promoter region as described in Figure 2. Values are normalized to the PCR product corresponding to the *PHO5* TATA region, which is defined as 100. Data are presented as the average of three independent experiments along with the SEM.

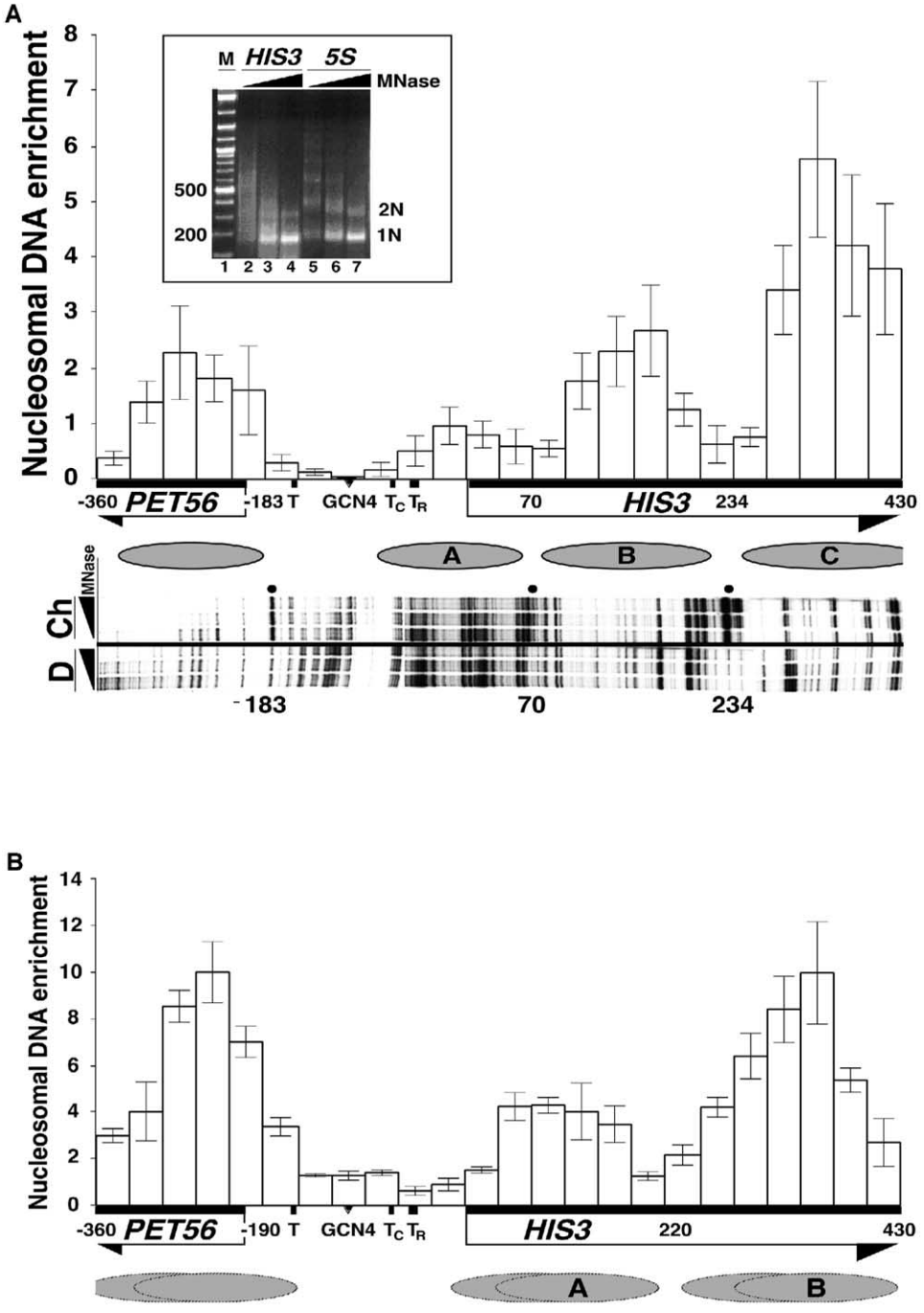

Figure 5. The *HIS3-PET56* Promoter Region Is Refractory to Nucleosome Formation In Vitro and In *Schizosaccharomyces pombe*

(A) A 2789 bp PCR-generated *HIS3-PET56* DNA fragment and a control fragment containing 5S rDNA repeats were reconstituted with HeLa core histones by gradient salt dialysis and digested with MNase, (inset; 1N and 2N represent mono- and dinucleosomes, respectively). The array assembled on the 5S template was 90% saturated with histones as determined by EcoRI digestion, and the amount of nucleosome monomers in the 5S and *HIS3-PET56* samples was comparable. Nucleosome DNA enrichment at the indicated positions was determined by nucleosome scanning as described in Figure 2. Shown below is an analysis of the same samples by amplified primer extension to reveal lower-strand cleavage profiles.

(B) Nucleosome scanning of an *S. pombe* strain containing the *HIS3-PET56* DNA region integrated at the *ura4* locus. Potential positioned nucleosomes are indicated by shaded, broken ovals.

Data are presented as the average of three independent experiments along with the SEM.

shifted ~30–50 bp from their major positions in vivo, again suggesting that cellular factors are involved in establishing preferred nucleosome positions in the *DED1* coding region. Most importantly, however, our results demonstrate that intrinsic histone-DNA preferences are primarily responsible for low nucleosome

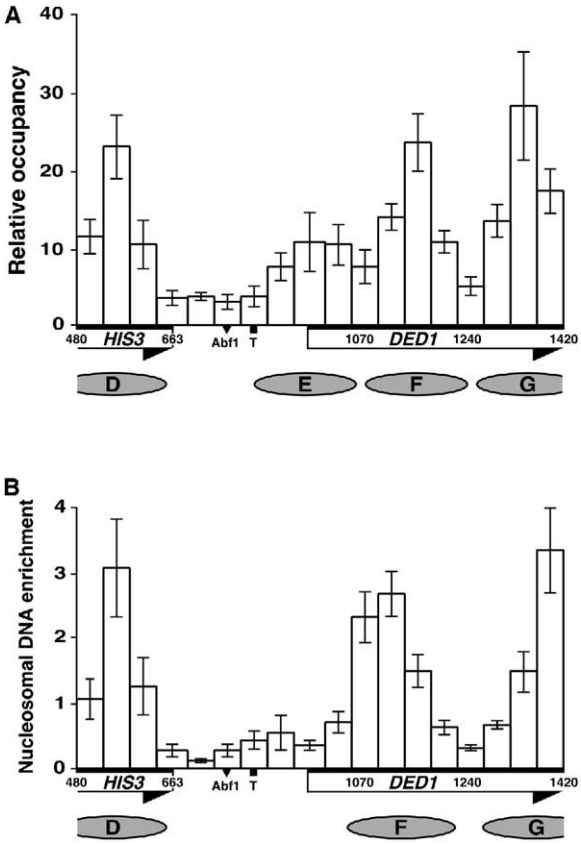

Figure 6. Intrinsic Histone-DNA Interactions Are the Primary Determinant of Low Histone Density at the *DED1* Promoter Region

(A) Nucleosome scanning of the *DED1* promoter region in vitro using the sample described in Figure 5A.

(B) Nucleosome-scanning analysis of the *DED1* promoter region in vivo using samples and techniques described in Figure 2.

Data are presented as the average of three independent experiments along with the SEM.

density of the *HIS3-PET56* and *DED1* promoter regions in vivo.

Low Histone Density Is a Very Common Feature of Yeast Promoter Regions that Is Unrelated to Transcriptional Activity

To address whether histone density of promoter regions is low relative to the adjacent coding regions, we first analyzed 23 randomly chosen genes for levels of histone H4 occupancy. In this experiment, ChIP was performed by conventional methods, meaning that the average lengths of crosslinked DNA and PCR fragments were ~400 and 250 bp, respectively. As a consequence, histone density is effectively being averaged over regions containing several nucleosomes, which will minimize potential differences between promoters and coding regions. Nevertheless, 83% (19/23) of the regions studied had significantly reduced levels of histone H4 at their promoter relative to the coding region (Figure 7A; left). The average density of promoter regions was 3.35-fold lower than coding regions. Moreover, the low density of promoter regions is unrelated to transcriptional activity. Many genes with low density are very poorly transcribed, and *RPS11B* has high histone density at the promoter yet is highly transcribed.

We further analyzed histone H4 density on a genome-wide level by using microarrays containing essentially all intergenic regions or containing essentially all protein-coding regions (see Supplemental Data available with this article online). Given the size of the DNA fragments on the array, this approach averages histone density over regions that are 200–1000 bp, depending on the locus. H4 densities on the two different arrays were calibrated relative to the density of *PHO5* promoter and *PHO5* coding region, which were arbitrarily set to 1.0. The array data are valid, because the behaviors of the 23 randomly selected DNA regions on the array are very similar to what was observed by direct analysis (Figure 7A, right). Importantly, out of 4331 genes where data for both promoter and coding regions are reliable, 3142 (72.6%) coding regions contain $\geq$2-fold higher H4 levels than the adjacent promoter (Figure 7B). In contrast, only 24 genes (0.5%) showed $\geq$2-fold higher histone octamer levels at promoters as compared to coding regions. Thus, the majority of yeast genes show significantly lower levels of histone content relative to their corresponding coding region.

On a genome-wide basis, reduced H4 density at promoters with respect to their corresponding coding regions is unrelated to transcriptional activity (Figure 7C). First, the vast majority of genes with reduced H4 density at promoters are transcribed at low levels (values below 20 in Figure 7C). Second, the distribution of promoter:coding ratios of H4 density in poorly transcribed genes (values below 20) is indistinguishable from that of more actively transcribed genes (values above 20). For both classes of genes, median values are ~0.5, and 50%–80% of all genes within any given transcriptional range show at least a 2-fold reduction in H4 density at promoters. Third, an expected number of highly transcribed genes do not show reduced H4 density at promoters. Our results are in excellent accord with a recent report that was published after this work was initially submitted (Lee et al., 2004). In particular, the transcription-independent phenomenon of lower histone density at promoters versus their corresponding coding regions is distinct from the transcription-dependent effects on reduced histone densities at promoters (presumably due to activator-mediated eviction) or at coding regions (presumably due to disruption by elongating RNA polymerase II). Thus, genomic analysis supports the view that low histone density at most promoters is strongly influenced by intrinsically weak histone-DNA interactions.

Discussion

Most Yeast Promoter Regions Have Low Nucleosome Density

A large body of evidence indicates that yeast promoter regions are generally more accessible than protein-coding regions. In a number of cases, preferential accessibility is unrelated to transcriptional activity, and standard MNase mapping reveals the apparent absence of positioned nucleosomes. Here, we use two methods to show

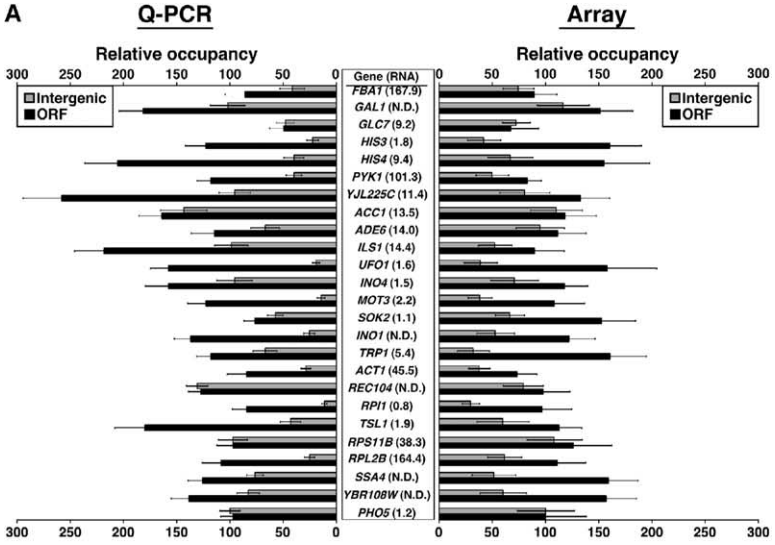

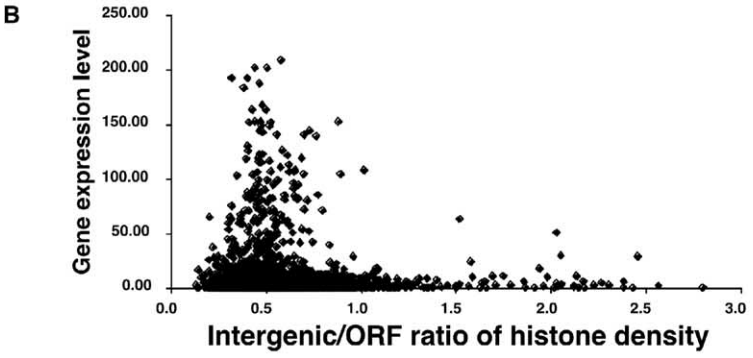

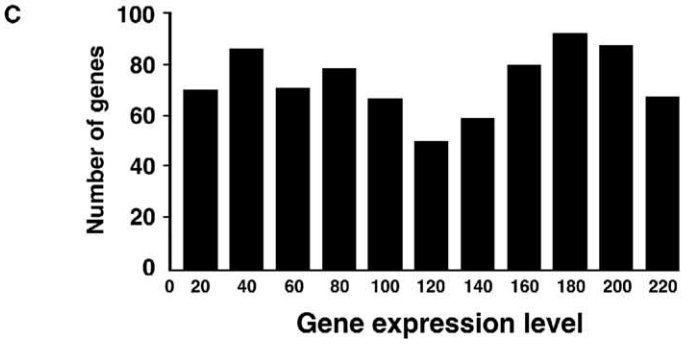

Figure 7. Most Promoters Have Lower Histone Density Than Their Corresponding Coding Region

(A) Data are represented as H4 content normalized to the *PHO5* intergenic primer pair that was arbitrarily set to 100 (left). Transcriptional frequency values are defined as the number of RNA molecules produced per hour (Holstege et al., 1998); N.D. means RNA not detected. Right, analysis of the same genes on the whole-genome microarrays containing either intergenic regions or coding regions; H4 levels are relative to the *PHO5* intergenic or ORF region that were arbitrarily set to 100. Data are presented as the average of three independent experiments along with the SEM.

(B) The ratio of histone density of a given promoter with respect to its corresponding coding region is plotted as a function of gene expression level.

(C) The percent of genes with low histone density at the promoter with respect to the corresponding coding region (defined as a ratio of <0.5) is plotted with respect to the indicated bins of gene expression level.

that histone density in the *HIS3-PET56* promoter region is <10% of the flanking coding sequences. Furthermore, histone density in the immediately adjacent coding regions is significantly below full occupancy, even though positioned nucleosomes flank the intergenic region.

By directly measuring histone H4 occupancy in a manner that does not depend on MNase cleavage, we also show that low nucleosome density is a very common feature of yeast promoter regions. Strikingly, 83% (19/23) of randomly chosen genes have reduced levels of histone H4 at their promoter relative to the coding region, with the average density of promoter regions being about 3-fold lower than coding regions. Genome-wide analysis directly demonstrates that many yeast promoters are deficient in nucleosomes. Aside from

providing further support for the low density of nucleosomes in the 5′-proximal coding regions, this observation is remarkable because the analysis is performed on DNA fragments that average approximately three nucleosomes in length. Thus, 500 bp regions in the vicinity of the many promoters contain, on average, only one nucleosome at any given time. Thus, yeast promoter regions do not only contain short nucleosome-free regions but also are often deficient in nucleosomes over surprisingly extended regions. The generality of this phenomenon as well as analysis of individual genes on a genome-wide basis indicates that such nucleosome deficiency is unrelated to transcriptional activity.

Preferential Accessibility of the *HIS3-PET56* and *DED1* Promoter Regions Is Primarily Determined by the Intrinsic DNA Sequence Specificity of Histones

The observation that the wt *HIS3-PET56* promoter region is nearly devoid of nucleosomes strongly suggests that preferential accessibility arises simply from reduced competition by histones. Progressive deletion of the promoter region in either direction results in a progressive loss of accessibility to HinfI cleavage in vivo (Mai et al., 2000), and we show here that these deleted derivatives differ with respect to histone density. Specifically, the length of the nucleosome-deficient region is reduced, the level of histone density is increased in the remaining part of the promoter region, and the discrimination between the promoter region and the neighboring nucleosome is less pronounced. Furthermore, the severity of these effects increases in accord with the extent of the deletion. This strong relationship between nucleosome occupancy and the level of HinfI cleavage in vivo provides direct experimental evidence that preferential accessibility of the divergent *HIS3-PET56* promoter region is due primarily to lack of competition with histones. As linker regions in *S. cerevisiae* are typically short (20–30 bp), relatively large regions that show 2- to 3-fold reductions in histone density should have a major effect on protein accessibility.

The near absence of nucleosomes in the *HIS3-PET56* and *DED1* promoter regions in vivo is due to intrinsic DNA sequence preferences of histones, because low nucleosome density in this region is faithfully reproduced in vitro with purified histones and DNA. Furthermore, the *HIS3-PET56* promoter region is similarly devoid of nucleosomes in *S. pombe*, an evolutionarily distant yeast species. Intrinsic histone-DNA preferences also account for the position of the adjacent nucleosome over the *PET56* coding region and nucleosome D, which covers the 3′ end of the *HIS3* coding region. In contrast, the predominant positions of nucleosomes A, B, and C in the *HIS3* coding region and nucleosomes F and G in the *DED1* coding region are altered in vitro and in *S. pombe*, suggesting that nucleosome remodeling complexes (and perhaps other chromatin-modifying activities) are involved. Importantly, although intrinsic histone-DNA preferences do not account for all aspects of nucleosome positioning in vivo, they are sufficient to explain low nucleosome density at the *HIS3-PET56* and *DED1* promoter regions.

Detailed analysis of the divergent *HIS3-PET56* promoter region indicates that preferential accessibility does not depend on specific genetic elements but rather is determined by a general property of the DNA sequence over a 150–200 bp region (Mai et al., 2000). This unusual genetic requirement for preferential accessibility is nicely explained by the fact that low nucleosome density in the *HIS3-PET56* promoter region results from intrinsic histone-DNA preferences. Intrinsic nucleosome positioning is significantly determined by preferences for DNA sequence periodicities that are related to DNA bending (Drew and Travers, 1985; Satchwell et al., 1986; Sivolob and Khrapunov, 1995; Lowary and Widom, 1998; Thastrom et al., 1999; Thastrom et al., 2004). For example, the minor grooves of AAA and AAT face inward toward histones, whereas those of GGC and AGC face outward. More generally, the stability of a nucleosome at any particular position reflects a cumulative accounting of positive and negative interactions that occur as the DNA curves around the histones (Widom, 2001). Thus, DNA regions with intrinsic low nucleosome density must have sequence characteristics that extend over a length that approximates the size of a nucleosome itself. Thus, the "general property" of the nucleosome-sized region that governs preferential accessibility (Mai et al., 2000) is very likely to be directly related to an intrinsically poor ability to form a stable nucleosome.

Implications for Binding of Transcriptional Regulatory Proteins to Target Sites in Physiological Chromatin

As DNA binding activator and repressor proteins typically recognize short sequence motifs that occur many times in the genome, cells must possess a mechanism whereby irrelevant binding sites are relatively inaccessible in comparison to sites in target promoters. There are several mechanisms to generate accessible regions in promoters. First, a short nucleosome-free region will arise if two well-positioned nucleosomes are spaced too closely together to allow the formation of a nucleosome between them (Terrell et al., 2002). Second, binding of an activator protein to a specific site can create larger regions of preferential accessibility (Devlin et al., 1991; Gross et al., 1993). In these and other cases, it is likely that the activator protein recruits nucleosome-remodeling and other chromatin-modifying complexes to the promoter, thereby increasing accessibility in a localized manner. Third, as exemplified by the *HIS3-PET56* and *DED1* promoter regions analyzed here, accessibility reflects relatively large regions of DNA that intrinsically interact poorly with histones.

Although short, internucleosomal regions and activator-specific alteration of nucleosomes can facilitate binding the proteins to their target sites in promoters, our results strongly suggest that an important mechanism for preferential accessibility is that promoters contain DNA sequences with poor nucleosome-forming potential. Short regions between positioned nucleosomes are unlikely to be specific to promoter regions, and they cannot explain the low levels of histone density observed at a significant majority of promoters. Activator-specific alterations of nucleosomes in the promoter region are unlikely to be a general mechanism,

because the vast majority of yeast genes are poorly transcribed under standard conditions, and activator proteins are required for high levels of transcription. In addition, activator-dependent disruption of chromatin does not account for how activators selectively disrupt nucleosomes in promoter regions as opposed to coding regions with consensus binding sites. However, activator-mediated eviction of promoter nucleosomes will clearly be facilitated by intrinsic histone-DNA interactions that result in preferentially low histone density at promoters with respect to coding regions.

Our results strongly suggest that the yeast genome is not fully coated with nucleosomes in a "beads-on-a-string" manner but rather is organized into distinct promoter and nonpromoter regions, whose DNA sequences inherently differ with respect to nucleosome formation. A remarkable aspect of this organization is that evolutionary pressure to maintain this important functional property is applied to relatively large regions of DNA (typically at least the length of a single nucleosome) rather than to short sequence motifs. Many different sequences can serve this "nucleosome-inhibiting" function, and there is likely to be considerable evolutionary drift in sequences even among closely related yeast species. In this regard, it is almost certain that predictions about which genomic regions have low nucleosome density will be impossible from DNA sequence comparisons among genes and organisms but rather will require detailed understanding of the energetic contributions of specific interactions between base pair combinations and histones.

Because transcriptional regulation depends on numerous proteins, low nucleosome density should improve accessibility of multiple proteins that interact directly with promoter DNA. As a consequence, preferential accessibility of promoter regions should result in a synergistic effect on transcription from promoters as opposed to coding regions. Examples of synergistic effects that do not depend on transcriptional activation domains have been observed in yeast cells (Oliviero and Struhl, 1991; Miller and Widom, 2003). However, low nucleosome density in the *HIS3-PET56* promoter region per se is insufficient for transcription (Mai et al., 2000), indicating that the basic RNA polymerase II machinery functions poorly in vivo even when the core promoter is quite accessible. Thus, although transcriptional activator proteins can make promoter regions more accessible by recruiting chromatin-modifying activities, recruitment of the basic RNA polymerase II machinery is not passive and must require direct effects of the activator. Nevertheless, the intrinsic structural distinction between promoter and nonpromoter regions effectively reduces the concentration of inappropriate binding sites and, hence, provides an important mechanism to restrict transcriptional initiation to promoters.

Experimental Procedures

Yeast Strains and DNAs

Saccharomyces cerevisiae strains used in this study have been previously described (Mai et al., 2000) and were cultivated at 30°C in either YPD medium supplemented with 0.04 mg/ml adenine or synthetic complete medium lacking tryptophan or uracil. For experiments involving epitope-tagged histone H4, strains were transformed with pNOY436 (*CEN6*; *TRP1*, *HHT2*, and *myc-HHF2*) generously provided by M. Nomura (Keener et al., 1997). Targeting of the *S. cerevisiae PET56-HIS3* region to the chromosomal *ura4* locus of the *Schizosaccharomyces pombe* strain WP17 (*ura4.595*) (van Heeckeren et al., 1998) was accomplished by using the *S. pombe* integrating vector pJK210 (ATCC 86958) containing a 2789 bp *PET56-HIS3* PCR product (–1209 to +1580 relative to the *HIS3* ATG). The resulting DNA molecule pES14 was cleaved with StuI, located at position +399 relative to the *ura4* ATG, and integrated in single copy into WP17 cells to generate *S. pombe* strain EAS16.

MNase Digestion of Chromatin and Purified DNA

MNase digestion of chromatin was performed on spheroplasts by using a procedure that minimizes the time after the isolation of intact cells (Kent and Mellor, 1995). Exponentially growing cells (200 ml) were washed with 1 M sorbitol and resuspended in 1 ml of spheroplasting buffer (1 M sorbitol, 1 mM β-mercaptoethanol, and 50 mg/ml lyticase [ICN]) for 8 min at room temperature. Spheroplasts were washed two times with 1 M sorbitol, and the pellet was resuspended with 1 ml digestion buffer (1 M sorbitol, 50 mM NaCl, 10 mM Tris [pH 7.4], 5 mM $MgCl_2$, 1 mM $CaCl_2$, 1 mM β-mercaptoethanol, 0.5 mM spermidine, and 0.075% NP-40). 250 μl aliquots were treated with 0, 60, 120, or 240 U/ml of MNase (USB) for 5 min at 37°C, whereupon the reaction was terminated with 1/10 volume of 250 mM EDTA and 5% SDS. RNA and proteins are degraded, and the resulting, purified genomic DNA was subjected to analysis. To generate control samples of genomic DNA, 24 μg of *S. cerevisiae* DNA, purified with a Qiagen genomic DNA isolation kit, were added to a 200 μl reaction (2 mM $CaCl_2$, 5 mM $MgCl_2$, and 40 mM HEPES [pH 7.5]), divided into four 50 μl aliquots, and treated with 0, 15, 30, or 60 mU of MNase. Genomic DNA samples were Qiagen-column purified and subjected to analysis.

Low- and Nucleotide-Level Mapping of MNase Cleavage Sites by Indirect End Labeling

Standard, low-level mapping of MNase cleavage sites was performed by Southern blotting. MNase-treated DNA was cleaved with Asp714, electrophoretically separated on a 2% agarose gel (10 μg/lane), and blotted by alkaline capillary transfer to nylon. The transferred DNA was UV crosslinked and then hybridized at 65°C with a *HIS3* DNA probe (+368 to +622) synthesized by random hexamer priming in the presence of 100 μCi ^{32}P-dATP. To map MNase cleavage sites at nucleotide resolution, 1 μg of MNase-treated genomic DNA was subjected to amplified primer extension essentially as described (Erkine et al., 1995). Radioactively end-labeled *HIS3*-specific oligonucleotides employed in this study were: 5′-GGTTTC ATTTGTAATACGCTTTACTAGGGC-3′ (spanning nucleotides +68 to +39) and 5′-GCAAATCCTGATCCAAACCTTTTTACTCC-3′ (spanning nucleotides +388 to +360) to reveal lower-strand analysis.

Nucleosome-Scanning Analysis

MNase-treated chromatin and purified DNA samples were electrophoretically separated on a 1.5% agarose gel, and mononucleosome-sized (140–220 bp) fragments were excised from the gel and purified (Qiagen column). The resulting material was analyzed by a set of overlapping primer pairs, each of which generate 100 ± 8 bp PCR products that are located 30 ± 10 bp away from neighboring primer pairs. PCR efficiency for each primer pair was within 0.5 cycles of a dedicated primer pair for either *HIS3* or *PHO5*, as assayed with genomic DNA and detected by quantitative PCR.

ChIP

For some experiments, formaldehyde-crosslinked chromatin was fragmented by sonication by standard methods (Aparicio et al., 2004). For experiments involving mononucleosomes, fragmentation of crosslinked protein-DNA complexes was accomplished by extensive MNase digestion using the following modifications. Prior to sonication, the cell lysate (1×10^8 cells; 50 mM HEPES [pH 7.5], 150 mM NaCl, 1 mM EDTA, 1% Triton X-100, 0.1% sodium deoxycholate, 0.1% SDS, and 1 mM PMSF) was adjusted to 20 mM $MgCl_2$, 5 mM $CaCl_2$, 300 μg RNAase A and digested with either 0, 450, 1350, or 4050 U of MNase for 30 min at 37°C. Termination is achieved by 1/50 volume of 0.5 M EDTA. From this point, the stan-

dard protocol was followed with the sonication step required to solubilize the MNase-fragmented chromatin. Chromatin generated by either procedure was immunoprecipitated with c-Myc (9E10) mouse monoclonal IgG_1 antibody (Santa Cruz Biotechnology, Inc) or rabbit polyclonal antibody to histone H3 that recognizes the C-terminal core domain (Abcam).

In Vitro Reconstitution Experiments

Gradient salt dialysis was used to assemble nucleosome arrays on a 2789 bp *HIS3-PET56* DNA fragment generated by PCR (–1209 to +1580 relative to the *HIS3* ATG) and a control 2546 bp fragment (G5E4) with five 5S rDNA positioning sequences flanking a ~400 bp sequence containing five Gal4 binding sites, the E4 promoter, and several unique restriction sites with the central 400 bp segment accommodating two nucleosomes (Neely et al., 1999). The procedure was modified from Luger et al. (1997), and all steps were performed at 4°C. 35 μg of each DNA were incubated in 50 μl reactions containing 20 mM Tris-HCl (pH 7.7), 10 mM DTT, 0.5 mM EDTA, 2 M NaCl, 0.5 mM benzamidine, and 31.5 μg of purified HeLa core histones (added last). Samples were placed in a microdialysis apparatus with 6–8 kDa dialysis tubing previously boiled in distilled water for 5 min. A Rainin Model RP-1 peristaltic pump assembly was used with 0.95 ml/min maximum flow rate tubing and a flow rate set at 200 μl/min (8.8 RPM). The samples were placed in a beaker containing 200 ml of high-salt buffer (20 mM Tris-HCl [pH 7.7], 2 M NaCl, 0.5 mM EDTA, 1 mM DTT, and 0.5 mM benzamidine), with the dialysis membrane contacting the buffer surface. With continuous stirring, high-salt buffer was gradually exchanged with low-salt buffer (same as above except with 250 mM NaCl) over a period of 72 hr. After this period, the low-salt buffer beaker was replaced with 200 ml of buffer lacking any NaCl, and the nucleosomes are further dialyzed for an additional 6 hr. Lastly, the nucleosome reaction vessel was placed directly into the buffer lacking NaCl for 3 hr with constant stirring.

The extent of nucleosome array assembly on the G5E4 DNA fragment was analyzed by EcoRI digestion (Carruthers et al., 1999) and determined to be 90% saturated with histones. The G5E4 and *HIS3-PET56* nucleosomal assembly mixtures were suspended in MNase-digestion buffer (20 mM Tris-HCl [pH 7.7], 0.5 mM EDTA, 1 mM DTT, 2 mM $CaCl_2$, 5 mM $MgCl_2$, and 40 mM HEPES [pH 7.5]) and then treated with 15, 30, or 60 mU of MNase. The amount of nucleosome monomers (quantitated after gel electrophoresis) in the G5E4 and *HIS3-PET56* samples was indistinguishable (<5% difference), indicating that nucleosome assembly on the *HIS3-PET56* template was very efficient. The resulting material was analyzed for in vitro nucleosome positioning by the nucleosome-scanning method and amplified primer extension.

Quantitative PCR Analysis

Quantitative PCR analysis in real time was performed by using either the Applied Biosystems 7700 or 7000 sequence detectors based on SYBR Green I fluorescence. Reactions were performed in 10 μl, and cycling was for 10 min at 95°C, followed by 40 cycles of 95°C; 30 s, 60°C; and 45 s, 72°C. The nucleosomal DNA enrichment level of a given DNA region was calculated as the ratio between the amounts of PCR product obtained from DNA samples generated from the mononucleosomal gel purification or immunoprecipitated chromatin experiments to that of the input (total) DNA. Ratios for deproteinized, MNase-treated DNA equivalent to the molecular mass of mononucleosomal DNA was similarly calculated and used for background subtraction. Additionally, the value obtained for the *PHO5* TATA control promoter region (designated primer pair PHO5.T) was arbitrarily set to 100, and all other in vivo nucleosomal DNA enrichment values are presented relative to this standard. In all figures, data are presented as the average of three independent experiments along with the SEM.

Microarray Analysis

MNase-generated, mononucleosomal-purified DNA 140–220 bp in length was amplified with random primers and hybridized to yeast intergenic and ORF microarrays, as previously described (Iyer et al., 2001; Moqtaderi and Struhl, 2004). Three biologically independent replicates were performed (two array set hybridizations per experiment). The signal intensity value obtained for each intergenic region and annotated ORF for each independent microarray were normalized to the median value, and the normalized median value for each genomic region was calculated. We arbitrarily set the value of histone density at the *PHO5* region to be 1.0, and all other values are determined relatively. The statistically significant signals were defined by the following parameters: (1) SEM must be $\leq$50% of the average signal intensity for a given spot, and (2) the average signal intensity for each spot must be greater than the average SEM value. The Spearman correlation coefficient for the rank order promoter:ORF histone densities of genomic loci for individual biological replicates was 0.61, indicating high reproducibility. Similar genome-wide results were obtained by using crosslinked, MNase-treated chromatin immunoprecipitated with c-Myc antibody. The ratio of histone density at the promoter with respect to its corresponding coding region was analyzed with respect to transcriptional activity (Holstege et al., 1998).

Supplemental Data

Supplemental Data include one table and are available with this article online at http://www.molecule.org/cgi/content/full/18/6/735/DC1/.

Acknowledgments

We thank Bob Kingston for the p2085S-G5E4 plasmid containing the linear array and purified HeLa histone core particles; Masayasu Nomura for the *myc-HHF2* plasmid; Geeta Narlikar, Hua-Ying Fan, and Antonin Tutter for technical advice involving the in vitro reconstitution assay; Joan Weiner for assistance with the microarray and quantitative PCR experiments; and Zhou Zhu for help with computational analysis. This work was supported by a postdoctoral fellowship award (GM064179) to E.A.S. from the National Institutes of Health (NIH) and by an NIH research grant to K.S. (GM30186).

Received: December 21, 2004
Revised: April 27, 2005
Accepted: May 5, 2005
Published: June 9, 2005

References

Anderson, J.D., Lowary, P.T., and Widom, J. (2001). Effects of histone acetylation on the equilibrium accessibility of nucleosomal DNA target sites. J. Mol. Biol. *307*, 977–985.

Aparicio, O.M., Geisberg, J.V., and Struhl, K. (2004). Chromatin immunoprecipitation for determining the association of proteins with specific genomic sequences in vivo. In Current Protocols in Molecular Biology, F.A. Ausubel, R. Brent, R.E. Kingston, D.D. Moore, J.G. Seidman, J.A. Smith, and K. Struhl, eds. (New York: John Wiley & Sons), pp. 21.3.1–21.3.17.

Becker, P.B., and Horz, W. (2002). ATP-dependent nucleosome remodeling. Annu. Rev. Biochem. *71*, 247–273.

Belotserkovskaya, R., Oh, S., Bondarenko, V.A., Orphanides, G., Studitsky, V.M., and Reinberg, D. (2003). FACT facilitates transcription-dependent nucleosome alteration. Science *301*, 1090–1093.

Boeger, H., Griesenbeck, J., Strattan, J.S., and Kornberg, R.D. (2003). Nucleosomes unfold completely at a transcriptionally active promoter. Mol. Cell *11*, 1587–1598.

Boeger, H., Griesenbeck, J., Strattan, J.S., and Kornberg, R.D. (2004). Removal of promoter nucleosomes by disassembly rather than sliding in vivo. Mol. Cell *14*, 667–673.

Carruthers, L.M., Tse, C., Walker, K.P., and Hansen, J.C. (1999). Assembly of defined nucleosomal and chromatin arrays from purified components. Methods Enzymol. *304*, 19–35.

Chen, W., Tabor, S., and Struhl, K. (1987). Distinguishing between mechanisms of eukaryotic transcriptional activation with bacteriophage T7 RNA polymerase. Cell *50*, 1047–1055.

Deckert, J., and Struhl, K. (2001). Histone acetylation at promoters is differentially affected by activators and repressors. Mol. Cell. Biol. *21*, 2726–2735.

Devlin, C., Tice-Baldwin, K., Shore, D., and Arndt, K.T. (1991). RAP1

is required for BAS1/BAS2- and GCN4-dependent transcription of the yeast HIS4 gene. Mol. Cell. Biol. *11*, 3642–3651.

Drew, H.R., and Travers, A.A. (1985). DNA bending and its relation to nucleosome positioning. J. Mol. Biol. *186*, 773–790.

Erkine, A.M., Adams, C., Gao, M., and Gross, D.S. (1995). Multiple protein-DNA interactions over the yeast HSC82 heat shock gene promoter. Nucleic Acids Res. *23*, 1822–1829.

Formosa, T., Ruone, S., Adams, M.D., Olsen, A.E., Eriksson, P., Yu, Y., Rhoades, A.R., Kaufman, P.D., and Stillman, D.J. (2002). Defects in SPT16 or POB3 (yFACT) in Saccharomyces cerevisiae cause dependence on the Hir/Hpc pathway. Polymerase passage may degrade chromatin structure. Genetics *162*, 1557–1571.

Gross, D.S., Adams, C.C., Lee, S., and Stentz, B. (1993). A critical role for the heat shock transcription factor in establishing a nucleosome-free region over the TATA-initiation site of the yeast *HSP82* heat shock gene. EMBO J. *12*, 3931–3945.

Holstege, F.C., Jennings, E.G., Wyrick, J.J., Lee, T.I., Hengartner, C.J., Green, M.R., Golub, T.R., Lander, E.S., and Young, R.A. (1998). Dissecting the regulatory circuitry of a eukaryotic genome. Cell *95*, 717–728.

Iyer, V.R., Horak, C.E., Scafe, C.S., Botstein, D., Snyder, M., and Brown, P.O. (2001). Genomic binding sites of the yeast cell-cycle transcription factors SBF and MBF. Nature *409*, 533–538.

Kaplan, C.D., Laprade, L., and Winston, F. (2003). Transcription elongation factors repress transcription initiation from cryptic sites. Science *301*, 1096–1099.

Keener, J., Dodd, J.A., Lalo, D., and Nomura, M. (1997). Histones H3 and H4 are components of upstream activation factor required for the high-level transcription of yeast rDNA by RNA polymerase I. Proc. Natl. Acad. Sci. USA *94*, 13458–13462.

Kent, N.A., and Mellor, J. (1995). Chromatin structure snap-shots: rapid nuclease digestion of chromatin in yeast. Nucleic Acids Res. *23*, 3786–3787.

Korber, P., Luckenbach, T., Blaschke, D., and Horz, W. (2004). Evidence for histone eviction in trans upon induction of the yeast *PHO5* promoter. Mol. Cell. Biol. *24*, 10965–10974.

Kristjuhan, A., and Svejstrup, J.Q. (2004). Evidence for distinct mechanisms facilitating transcript elongation through chromatin in vivo. EMBO J. *23*, 4243–4252.

Kuo, M.-H., vom Baur, E., Struhl, K., and Allis, C.D. (2000). Gcn4 activator targets Gcn5 histone acetyltransferase to specific promoters independently of transcription. Mol. Cell *6*, 1309–1320.

Lee, C.K., Shibata, Y., Rao, B., Strahl, B.D., and Lieb, J.D. (2004). Evidence for nucleosome depletion at active regulatory regulation genome-wide. Nat. Genet. *36*, 900–905.

Lee, D.Y., Hayes, J.J., Pruss, D., and Wolffe, A.P. (1993). A positive role for histone acetylation in transcription factor access to nucleosomal DNA. Cell *72*, 73–84.

Lieb, J.D., Liu, X.L., Botstein, D., and Brown, P.O. (2001). Promoter-specific binding of Rap1 revealed by genome-wide maps of protein-DNA association. Nat. Genet. *28*, 327–334.

Losa, R., Omari, S., and Thoma, F. (1990). Poly(dA)·poly(dT) rich sequences are not sufficient to exclude nucleosome formation in a constitutive yeast promoter. Nucleic Acids Res. *18*, 3495–3502.

Lowary, P.T., and Widom, J. (1998). New DNA sequence rules for high affinity binding to histone octamer and sequence-directed nucleosome positioning. J. Mol. Biol. *276*, 19–42.

Luger, K., Rechsteiner, T.J., Flaus, A.J., Waye, M.M., and Richmond, T.J. (1997). Characterization of nucleosome core particles containing histone proteins made in bacteria. J. Mol. Biol. *272*, 301–311.

Mai, X., Chou, S., and Struhl, K. (2000). Preferential accessibility of the yeast *his3* promoter is determined by a general property of the DNA sequence, not by specific elements. Mol. Cell. Biol. *20*, 6668–6676.

Martens, J.A., and Winston, F. (2003). Recent advances in understanding chromatin remodeling by Swi/Snf complexes. Curr. Opin. Genet. Dev. *13*, 136–142.

Mason, P.B., and Struhl, K. (2003). The FACT complex travels with elongating RNA polymerase II and is important for the fidelity of transcriptional initiation in vivo. Mol. Cell. Biol. *23*, 8323–8333.

Miller, J.A., and Widom, J. (2003). Collaborative competition mechanism for gene activation in vivo. Mol. Cell. Biol. *23*, 1623–1632.

Moqtaderi, Z., and Struhl, K. (2004). Genome-wide occupancy of the RNA polymerase III machinery in *Saccharomyces cerevisiae* reveals loci with incomplete transcription complexes. Mol. Cell. Biol. *24*, 4118–4127.

Nagy, P.L., Cleary, M.L., Brown, P.O., and Lieb, J.D. (2003). Genomewide demarcation of RNA polymerase II transcription units revealed by physical fractionation of chromatin. Proc. Natl. Acad. Sci. USA *100*, 6364–6369.

Narlikar, G.J., Fan, H.-Y., and Kingston, R.E. (2002). Cooperation between complexes that regulate chromatin and transcription. Cell *108*, 475–487.

Neely, K.E., Hassan, A.H., Wallberg, A.E., Steger, D.J., Cairns, B.R., Wright, A.P., and Workman, J.L. (1999). Activation domain-mediated targeting of the SWI/SNF complex to promoters stimulates transcription from nucleosome arrays. Mol. Cell *4*, 649–655.

Oettinger, M.A., and Struhl, K. (1985). Suppressors of *Saccharomyces cerevisiae* promoter mutations lacking the upstream element. Mol. Cell. Biol. *5*, 1901–1909.

Oliviero, S., and Struhl, K. (1991). Synergistic transcriptional enhancement does not depend on the number of acidic activation domains bound to the promoter. Proc. Natl. Acad. Sci. USA *88*, 224–228.

Reinke, H., and Horz, W. (2003). Histones are first hyperacetylated and then lose contact with the activated *PHO5* promoter. Mol. Cell *11*, 1599–1607.

Satchwell, S.C., Drew, H.R., and Travers, A.A. (1986). Sequence periodicities in chicken nucleosome core DNA. J. Mol. Biol. *191*, 659–675.

Schwabish, M.A., and Struhl, K. (2004). Evidence for eviction and rapid deposition of histones upon transcriptional elongation by RNA polymerase II. Mol. Cell. Biol. *24*, 10111–10117.

Sewack, G.F., Ellis, T.W., and Hansen, U. (2001). Binding of TATA-binding protein to a naturally positioned nucleosome is facilitated by histone acetylation. Mol. Cell. Biol. *21*, 1404–1415.

Sivolob, A.V., and Khrapunov, S.N. (1995). Translational positioning of nucleosomes on DNA: the role of sequence-dependent isotropic DNA bending stiffness. J. Mol. Biol. *247*, 918–931.

Struhl, K. (1982). Promoter elements, regulatory elements, and chromatin structure of the yeast *his3* gene. Cold Spring Harb. Symp. Quant. Biol. *47*, 901–910.

Terrell, A.R., Wongwisansri, S., Pilon, J.L., and Laybourn, P.J. (2002). Reconstitution of nucleosome positioning, remodeling, histone acetylation, and transcriptional activation on the *PHO5* promoter. J. Biol. Chem. *277*, 31038–31047.

Thastrom, A., Lowary, P.T., Widlund, H.R., Cao, H., Kubista, M., and Widom, J. (1999). Sequence motifs and free energies of selected natural and non-natural nucleosome positioning DNA sequences. J. Mol. Biol. *288*, 213–229.

Thastrom, A., Bingham, L.M., and Widom, J. (2004). Nucleosomal locations of dominant DNA sequence motifs for histone-DNA interactions and nucleosome positioning. J. Mol. Biol. *338*, 695–709.

Ura, K., Kurumizaka, H., Dimitrov, S., Almouzni, G., and Wolffe, A.P. (1997). Histone acetylation: influence on transcription, nucleosome mobility and positioning, and linker histone-dependent transcriptional repression. EMBO J. *16*, 2096–2107.

van Heeckeren, W.J., Dorris, D.R., and Struhl, K. (1998). The mating-type proteins of fission yeast induce meiosis by directly activating *mei3* transcription. Mol. Cell. Biol. *18*, 7317–7326.

Vettese-Dadey, M., Grant, P.A., Hebbes, T.R., Crane-Robinson, C., Allis, C.D., and Workman, J.L. (1996). Acetylation of histone H4 plays a primary role in enhancing transcription factor binding to nucleosomal DNA in vitro. EMBO J. *15*, 2508–2518.

Widom, J. (2001). Role of DNA sequence in nucleosome stability and dynamics. Q. Rev. Biophys. *34*, 269–324.

Accession Numbers

Raw microarray data are deposited in GEO under accession number GSE2659, and processed data are provided as Supplemental Data.